Qualitative Sagittarius A* Model Visual Properties

Alex Foster

July 14, 2026

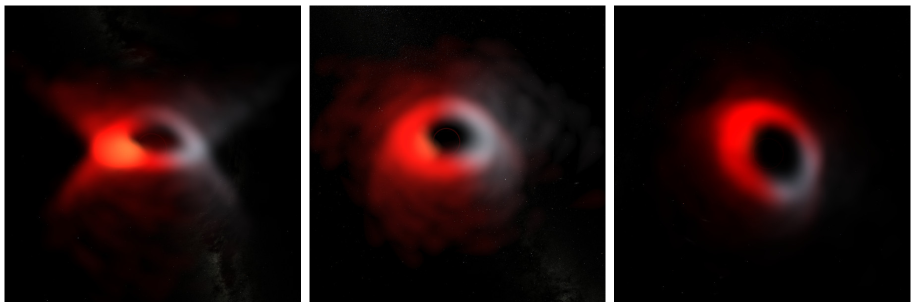

Figure 1: Images generated by the Sgr A* implementation running on the Nightshade G3 software. The image on the right uses $\gamma = 1$ to approximately match EHT image gamut. The images on the center and left use $\gamma = 2$. The backgrounds are not representative of the neighborhood of Sgr A*.

This paper discusses the qualitative properties and rendering techniques used to simulate the appearance of the black hole system Sagittarius A* (hereafter referred to as Sgr A*) from the perspective of a human viewer, specifically to fit within the constraints of Nightshade G3, Digitalis' universe simulation software for interactive planetarium use. The constraints on the observer properties lead to a different appearance than typical instrumentation would capture, and the real-time nature of the visualization imposes computational constraints on the model. The intent is to communicate the motivation behind visual and technical choices used in the model of Sgr A* that has been built for use in interactive planetarium systems.

Because direct visual-band measurement of Sgr A* is not available to closely constrain the models that are used to predict Sgr A*'s appearance, this paper will focus on the broad qualitative properties of the rendered model instead of specific quantitative values.

1 Color and Brightness

1.1 Observer Properties

The intent of this visualization is to capture the appearance that a human observer would have if they were placed at the camera location in the proximity of the black hole Sgr A*. The observer is assumed to have a neutral-density filter in the visual band such that they can comfortably see the image of the black hole system. The intensity of the accretion disk, even in the visual band where relatively little radiation occurs, would be dazzlingly bright to an observer within a few AU of the system.

We also assume that any non-visible radiation is blocked by a suitable filter. The radio and x/γ-ray emissions of a black hole accretion disk would quickly kill an unprotected human observer.

1.2 Luminosity

The color of a black hole is black, since light cannot escape. However, this does not mean that the system is dark; on the contrary, many black hole systems exceed the Eddington luminosity, the brightness at which an ordinary star would push itself apart as a result of the light pressing outwards. Sagittarius A* is relatively low luminosity by the standards of a supermassive black hole, but its overall energy output is still on the order of 10^{35} erg s^{-1} — many times that of our Sun.

Most of this radiation, however, is not visible to the human eye, as the synchrotron process emits radiation primarily in the radio and infrared frequencies. The visual-band luminosity of Sagittarius A* is still expected to be within about an order of magnitude as the Sun, at about 10^{32} erg s^{-1}. This output is more diffuse than the Sun, since the Sgr A* accretion disk region that emits most of the radiation is contained within about a 0.5 AU region (cf. solar diameter $\approx$ 0.01 AU).

From the distance of even the closest extrasolar stars[1], though, this relatively large size would still resolve as a point, since the largest stars are about $\frac{1}{20}$ of an arc second in diameter, about a thousand times smaller than a person with $\frac{20}{20}$ vision can resolve.[2]

1.3 Color

The visual band color of Sgr A* is likely dominated by two main processes, synchrotron radiation and inverse Compton scattering. Both rely on highly energetic relativistic particles in order to generate radiation within the visual band.

Synchrotron radiation is caused by particles traveling in curved trajectories at relativistic speeds. The majority of this radiation is in the radio and infrared wavelengths, with only the highest energy emission occurring in the visual band. The flux density caused by synchrotron radiation in the visual band declines from $\approx 10^{32}$ erg s^{-1} at 750nm to $\approx 10^{31}$ erg s^{-1} at 375nm. Visually, this is a deep red color, closer to pure red than a red black-body ($\approx$ 1500 K).

The second main contributor to the flux density at visible frequencies is the inverse Compton effect. This boosts the energy (and consequently reduces the wavelength) of photons that interact with relativistic particles (mostly electrons) orbiting in the accretion disk. This can occur multiple times for the same

[1] Note, however, that Sgr A* has much closer stars than the proximity of the Sun. The close star S2, for example, passes within about 120 AU (GRAVITY collaboration, 2018) of Sgr A*.

[2] $\frac{20}{20}$ vision is defined as sufficient acuity to resolve details at 1 arc minute angular size.

photon, but all higher order Comptonization of synchrotron photons result in particles with wavelengths too short to be visible.

The flux resulting from Compton radiation rises mildly with frequency inside the visible spectrum, leading to these photons having a pale bluish-white color. In the visible spectrum, however, this emission is buried underneath the base synchrotron radiation and therefore without any Doppler shift the color of the overall spectrum will remain red. The Compton radiation only takes over at the borderline between the visible spectrum and near ultraviolet. The Compton radiation flux is on the order of 3×10^{31} erg s^{-1} in the visual band, rising by a factor of around two from the near infrared to the near ultraviolet.

Both of these effects drop off superlinearly as particle velocities decrease, meaning that only the hottest particles near the event horizon emit substantial amounts of synchrotron or Comptonized synchrotron radiation. The majority of the emission from the black hole system is from within a few Schwarzschild radii of the event horizon.

1.4 Doppler Effect

Objects orbiting around the black hole have orbital velocities at appreciable fractions of the speed of light, resulting in the Doppler effect changing the effective radiation temperature of those objects. For an object orbiting at the innermost circular orbit at $3R_s$ the orbital speed is approximately $\frac{c}{2}$, and therefore the Doppler factor is $\sqrt{\frac{1+0.5}{1-0.5}} = \sqrt{3} \approx 1.73$.

Looking at the frequencies that are possibly visible with the assistance of Doppler shifting, we see a sharply dropping flux density between the near infrared and the edge of the visible range, and a slightly rising flux density from Comptonized photons starting at the purple end of the visible spectrum and rising into the near ultraviolet.

The u-shaped flux density predicted by the Event Horizon Telescope (EHT) collaboration (shown in Fig. 2) results in some counterintuitive properties when a Doppler shift is applied. Blueshifting the spectrum will allow more intense synchrotron radiation to be visible (making the image more red). Redshifting the spectrum will allow Comptonized photons to be visible as the base synchrotron radiation falls out of the visible band into the infrared. This means the approaching face of the black hole would be shifted towards the red, and the receding face towards the blue.

Because of the natural intensity increase caused by a blue shift, as well as the synchrotron radiation being much stronger in the near infrared than in the visible band, the approaching red disk region will be approximately 10^2 times brighter than the receding blue-white region.[3]

[3]However, the contrast constraints of available projection systems means that a contrast ratio this high is impractical for actual planetarium use.

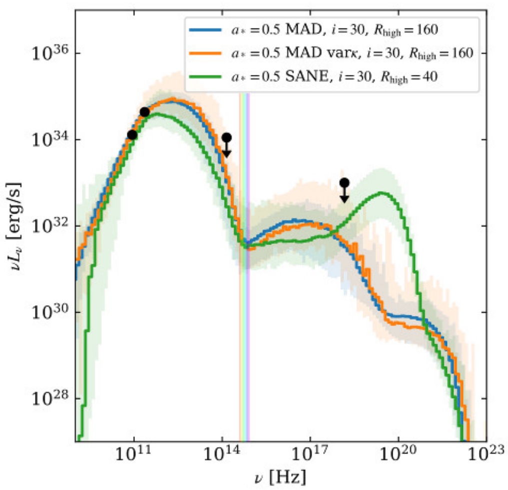

Figure 2: Modeled SED plots from the EHT collaboration (2022) (figure 10, CC-BY 4.0), with the visual band overlaid. Unlike a black-body source, the region near the visual band is expected to have a u-shaped distribution. The blue and orange lines represent the more favored models by the EHT papers.

1.5 Gravitational Redshift

The gravitational redshift, similarly to the Doppler effect, works to modify the effective color temperature of the black hole. Photons moving out of a gravity well lose energy, and photons traveling into one gain energy by a factor of $(1 - \frac{R_s}{r})^{-\frac{1}{2}}$. A particle at the innermost stable circular orbit at $3R_s$ being viewed from infinity would have a redshift factor of 1.22, resulting in a dimming of about 18 percent, and a slight shift downwards in frequency observed (note that as before, this will make the visible radiation bluer).

While 18% is a measurable amount, humans have a relatively difficult time noticing an 18% difference in light intensity. This effect slightly but broadly dims the bright core of the accretion disk, but is a relatively small factor compared to the Doppler effect, and far smaller than the increased emission intensity from relativistic particles at short radii. In γ-lighting space, the gravitational redshift at 3 R_s has approximately the same brightness change as the difference between (0.5, 0.5, 0.5) and (0.55, 0.55, 0.55).

1.6 Comparison with other visualizations

1.6.1 Color

The earliest depiction of black holes in their most commonly depicted color palette[4], which ranges from red-dark to white-hot, appears to be from illustrations made by Jean-Alain Marck and Jean-Pierre Luminet and published in 1997 in *Pour La Science*, a French science magazine. In it, the article describes that the red-orange-yellow-white color gradient chosen is of an arbitrary mapping of colors to luminosity, and does not indicate the physical color of the black hole disk. A similar gradient is used for the Event Horizon Telescope's M87* and Sgr A* images, which likewise use color to indicate luminosity and not spectral information.

This type of illustration is useful to indicate how effects like the relativistic Doppler effect cause the receding side of the disk to be less luminous than the approaching face, but does not correspond to how the disk would appear in the visual band, as could be implied by an observer.

1.6.2 Disk

Many visualizations use a two-dimensional accretion disk model. The biggest advantage of the 2D accretion disk is that it showcases the Schwarzschild metric much more clearly than the more diffuse models predicted by simulation. The 2D planar simulation is also much more straightforward to calculate and lends itself better to a fragment shader implementation, making it more straightforward to integrate into many rendering pipelines.

The disk simulation models that met the constraints of the EHT data, however, indicate that the strongly emitting parts of the disk are in a biconical configuration, with heart-shaped lobes extending significantly above and below the equatorial plane. This is the configuration adopted by the implementation of the Sgr A* model.

2 General Relativistic Effects

2.1 Overview

All paths that light travels along are curved by the presence of mass, whether by black hole, white dwarf, star, planet, or party balloon. However, most objects are insufficiently massive to make a noticeable change in the trajectory of light; the Sun is only able to deflect the light from a distant star by about 1.75 arc seconds. This is equal to about one pixel on a (completely infeasible) planetarium dome with a 370k resolution (107 gigapixels).[5]

[4] J.P. Luminet published their first accretion disk illustrations many years prior (Luminet 1979), with approximately the same luminosity mapping, but it appears this was not done in color.

[5] Typical commercial planetarium installations have resolutions on the order of 10 to 100 megapixels.

The intensity of the bending effect increases strongly as the light path draws closer to the mass that conducts the lensing, so *compact objects* like white dwarfs, neutron stars, and black holes are ideal candidates to not intersect the path of the light as it is being bent. These curved paths are *geodesics* and calculating their trajectory analytically is possible for a limited set of solutions to Einstein's field equations.

The simplest solution to the Einstein field equations that allows a matter distribution is the Schwarzschild metric. This admits a single point mass with no other massive objects at any other location, approximately describing a black hole system[6]. This solution is highly symmetric as there is no privileged orientation and as a result, all points at a given distance from the black hole have equivalent solutions (with the appropriate choice of coordinate system).

The Kerr solution to the field equations also allows the point mass to have angular momentum (spin). This solution is an extremely good approximation of the physics of a real black hole, but unfortunately adding spin results in several fewer dimensions of symmetry. This means the Kerr solution is not practical to calculate in real time, and as a result the Schwarzschild solution is preferred despite being a significantly worse analog for physical black holes.

The best-guess models for Sagittarius A* discussed by the EHT collaboration predict a spin parameter of $a_* = 0.94$, indicating a fast-spinning black hole aligned in spin direction with the accretion disk rotation (prograde rotation).

There exist solutions for black holes that have charge, or charge and spin, but physical black holes are expected to be neutral. A charged black hole would attract particles with the opposite charge until it becomes neutral again.

2.2 Approximate Schwarzschild Solution

The approximate solution for the Schwarzschild metric used by this simulation uses Beloborodov's cosine approximation:

$$1 - \cos\alpha = (1 - \cos\psi)(1 - \frac{1}{R}) \tag{1}$$

where α is the trajectory angle away from the black hole radial from an emitter E, defined by the angle ψ for an emitter E at the distance R (in units of Schwarzschild radii, R_s) from the black hole. The axis from which ψ is defined corresponds to the axis passing through the black hole which is parallel to the photon's path at the asymptotic limit far away from the black hole (where lensing is no longer occurring).

Finding the correct geodesic which passes through the camera and source position can be done using Beloborodov's method outlined above, solving to find the appropriate reference axis from which to define ψ from. This is possible by solving for the impact parameter b (the distance of the ψ reference axis from the asymptotic path of the light at large distances) which can be derived from Beloborodov's approximation:

[6]This is a good mass distribution approximation since the mass of the black hole is several orders of magnitude larger than its accretion disk.

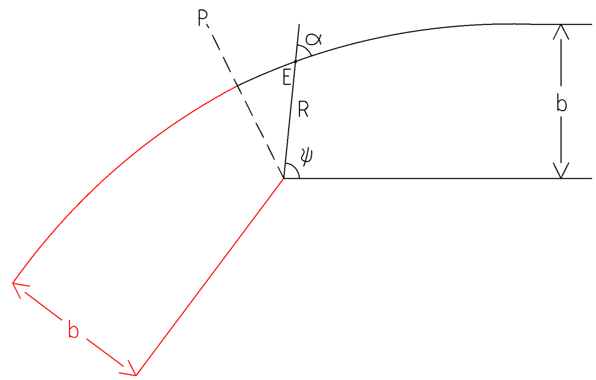

Figure 3: Coordinate system for the Beloborodov (2002) cosine approximation. To span the trajectory of a photon crossing the periapsis, the coordinate system can be mirrored (shown in red) across the periapsis axis (P).

$$b(\psi, r) = \sin\psi\sqrt{r^2 + r\cot\frac{\psi}{2}} \tag{2}$$

There exists some ψ such that the impact parameter b is the same for both the source and the camera, which can be calculated by using a root-finding algorithm to determine the value of ψ such that $b_s - b_c = 0$ (where b_s is the impact parameter of the source and b_c is the impact parameter of the camera). This method compensates for curvature at both the source and camera positions.

Beloborodov's approximation uses coordinates that do not span the entire trajectory of a photon approaching and diverging to infinite distance. Two adjoining coordinate systems (Fig. 3) are needed to build Beloborodov's approximation into a solution that spans this entire trajectory, joined at the periapsis (location of closest approach). This can be found by the following equation (Poutanen 2020), where b is found by Eq. 2:

$$p = -\frac{2b}{\sqrt{3}}\cos\frac{\arccos\left(\frac{3\sqrt{3}}{2b}\right) + 2\pi}{3} \tag{3}$$

Calculating trajectories is greatly aided by the symmetry conditions of the Schwarzschild metric. With no black hole spin vector to account for, there is no privileged orientation of source and observer positions relative to the black hole. Additionally, since no transverse frame-dragging effects exist, the photon trajectories always remain on the plane passing through the source, observer, and singularity points. This means that calculating the trajectory can be performed in two-dimensional polar coordinates and transformed freely to whatever three-dimensional coordinate system is desired.

This approximation for the light paths around a black hole is very accurate above about $r > 3R_s$ and deteriorates as the radius gets smaller than that. Fortunately the bulk of the accretion disk (as well as the rest of the Universe) is outside this radius, so this approximation provides a good fit for the trajectories being lensed for accretion disk visualization.

2.3 Shader Properties

The vertex shader works in the forward direction, by lensing paths from sources to find where they would be projected in the camera space. This is the inverse of other common lensing algorithms (e.g. by Bruneton (2020)), which start from an apparent position in camera space and then calculate intersections with the scene geometry. The latter method is suitable for a fragment shader, while the method proposed here is suitable for a vertex shader implementation, which has two important advantages:

- *Resolution scaling* — There are usually at least an order of magnitude less vertices in a scene than pixels. This ratio gets even higher for large planetarium systems above 4096 pixels in diameter, as the number of vertices remains relatively constant while the pixel count goes up with the square of the linear resolution. Calculating warping for millions of pixels per frame is a significant performance handicap when designing for systems with 20+ megapixel resolution.
- *Pixel smearing* — When a warping shader is applied to a texture, the resulting output image will tend to smear individual pixels into multiple pixels of lower brightness. If the pixels are sampling a background of the same resolution as the pixel pitch, this is not a problem, since lensing will distort the output image. However, practical stellar background textures are at resolutions far below that of the stars they represent, and so any distortion of distant point sources would be far below one pixel in size. Warping vertices directly obviates this concern, since even single precision floating point values are much more precise than any practical texture size.

2.4 Close-range Structure

In the Schwarzschild metric, the region from 1 R_s to 3 R_s is the region at which massive particles cannot orbit in circular orbits due to relativistic effects. This means that particles in this region must either cross the event horizon (defined as 1 R_s) or be expelled in erratic orbits or on hyperbolic departing trajectories. As a result, regardless of the accretion disk structure, little matter is expected to be inside of this region regardless of the accretion disk shape.

At the distance of exactly 1.5 R_s it is possible for photons to orbit the black hole in circular orbits. Photons traveling along the *photon sphere* cannot be seen since they are trapped in a bound orbit, but perturbations in spacetime caused by e.g. infalling matter may perturb them outwards on an approximately hyperbolic trajectory towards an outside observer. This will manifest as an image emanating from a ring surrounding the event horizon at approximately 1.5 R_s. Because of the curved geodesics in the proximity of the black hole, the apparent inner diameter of the accretion disk will be larger, at approximately the shadow diameter of $\frac{\sqrt{27}}{2} R_s$ (this will decrease towards 1.5 R_s at short distances).

3 Accretion Structure

The innermost few Schwarzschild radii around the black hole are where the majority of emission will take place. The EHT results for Sgr A* favor a disk with a heart-shaped cross-section, with emission primarily coming from a small region along the centerline as well as a lobe above and below the equatorial plane. Most of the emission occurs at less than 5 Schwarzschild radii, and given that the frequency of emission will tend to fall at larger distances from the black hole, the visible-band emissions may be even more compact than the model described by the EHT.

The most favored disk solution is the MAD (magnetically arrested disk) model, which involves general relativistic magnetohydrodynamic (GRMHD) forces beyond the scope of this simulation. The model used here is a simple morphological analog of the results found by the EHT.

The Sgr A* system has a relatively low intrinsic luminosity of about 10^{35} erg s^{-1}, multiple orders of magnitude below the Eddington limit for a black hole of its size. As a result, the Sgr A* system has a relatively small accretion region and does not contain a large jet structure (such as the one emitted from M87*).

4 Implementation

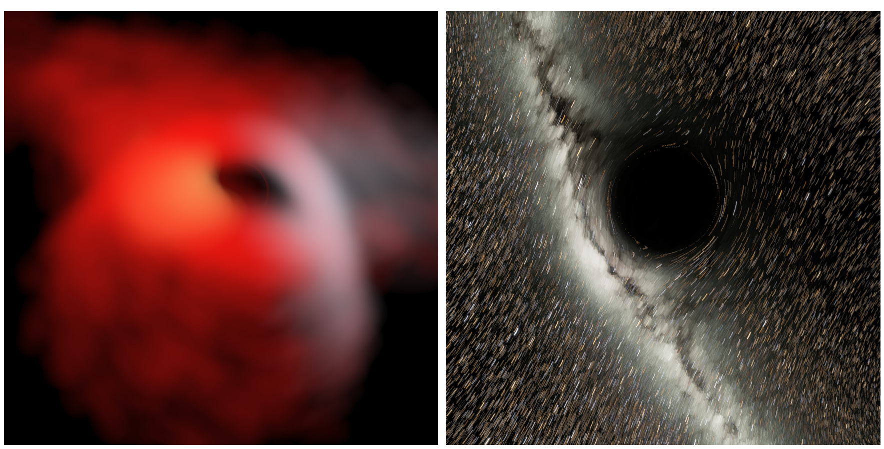

Figure 4: Images of Sagittarius A* (left) and black hole candidate Gaia18ajz (right), as rendered in Nightshade G3. The rendering of Gaia18ajz (which has no known accretion disk) is included with a trail effect to help make the background lensing effect more apparent.

The black hole model implementation uses a vertex shader transform based on Beloborodov's method (described above) and a particle-based accretion disk model. Each particle, representing a volume of the accretion disk, gets its color and intensity properties set by the vertex and geometry shaders. The position and direction of the particle is used to calculate the Doppler-adjusted color and shape of the particle.

The particles follow simple trajectories at constant distance from the polar axis, so their orbits are circular. This represents the group velocity of objects at that distance, as at any given latitude above or below the black hole, there will be an equal population of particles (save for the inwards drift towards the event horizon) rising away towards apoapsis as drifting back towards the periapsis in their elliptical orbits.

The images of the black hole in Fig. 4 are represented in the fisheye viewport used for planetarium projection. The diagonal field of view is approximately 160° and the horizontal and vertical fields of view are approximately 110°. The approaching side of the accretion disk is on the left of the images. Setting an appropriate camera position and reducing the γ of the image (rightmost image) to more closely match the output palette of the EHT imagery, we can see an image that is morphologically similar to that captured by the EHT collaboration.

5 Visualization Accuracy

- *Luminosity* — The luminosity that is apparent on a projector unfortunately cannot accurately describe the amount of contrast that the disk would have with the background, or with the outer parts of the disk. The visualization as drawn has a maximum contrast of about 1000:1 in 10-bit color; the contrast ratio of different parts of an accretion disk can be in the realm of 10,000:1 or more.

- *Color* — The color of the visualization should be relatively accurate, though there are the intrinsic limits of the available display technology. In particular, highlights become color-shifted (towards teal, yellow, purple, or white) because displays using RGB cannot create as much intensity in e.g. R as in R+G.

- *Doppler Shift* — The Doppler effect is approximately modeled to the extent that the limited luminosity range of the projection system can handle. In γ space this is a large increase in brightness for the approaching side of the disk. The u-shaped frequency distribution leads to the approaching side of the accretion disk to appear brighter and more red as infrared synchrotron radiation becomes more visible, and the receding side of the accretion disk to become bluer as the bright synchrotron radiation is redshifted out of the visual band.

- *Gravitational Redshift* — Not modeled. This effect is too small to be easily noticeable for $r > 3R_s$ where the disk lies. Where it is strong enough to cause a significant change in apparent color, at distances below $1.5R_s$, the luminosity is so low that it falls below the contrast floor outlined above.

Limitations in the domain of the lensing algorithm at present means that blueshift of the outside stars would also be too small to be noticeable.

- *Lensing* — The lensing implemented at present has a few main limitations compared to the exact Schwarzschild metric (which itself is a major simplification). First, the Beloborodov approximation has poor accuracy below 3 R_s (fortunately, the accretion disk is expected to be largely outside this radius). Second, only the least bent of two possible coherent solutions is imaged; in reality, there will be two coherent images of any given omnidirectional point source, one inside of and one outside of the Einstein radius. Currently the area inside the Einstein radius is black when it should contain another set of background images.

- *Accretion Disk* — The accretion disk shape approximates the best-guess models evaluated by the EHT Collaboration. The expected shape of the strongly emitting part of the accretion disk approximates an hourglass, with strong emission from a center ring and lobes above and below the equatorial axis. The disk is homogeneous with respect to angle around the polar axis, and no attempt has been made to calculate clumping or asymmetry in the disk.

- *Photon Ring* — The photon ring is round (Schwarzschild approximation) and of approximately the appropriate size. The intensity is unknown but likely not very high, as the EHT data does not prominently feature it in its models. A photon ring around a Kerr black hole has complex anisotropy and is not modeled. See illustrations in Abramowicz & Fragile (2013) for comparison to models using Kerr geometry.

- *Background* — The use of a vertex shader means that the stars drawn in the background are appropriately point-like despite the lensing effect. The images of the stars are warped, but at a scale far smaller than a single pixel.

6 References

1. Abramowicz, M. & Fragile, P. *Foundations of Black Hole Accretion Disk Theory* Living Rev. Relativ. 16, 1 (2013). https://doi.org/10.12942/lrr-2013-1

2. Abramowicz, M. et al. *Leaving the ISCO: the inner edge of a black-hole accretion disk at various luminosities* 2010, A&A 521, A15

3. Abramowitz, M. & Stegun, I. *Handbook of Mathematical Functions* 1970, ISBN 486-61272-4

4. Barbara, R. *Radiative Gas Dynamics*

5. Bruneton, E. *Real-time High-Quality Rendering of Non-Rotating Black Holes* 2020, arXiv:2010.08735

6. Beloborodov, A. M. *Gravitational Bending of Light Near Compact Objects* 2002, ApJ 566, L85

7. Dodelson, S. *Gravitational Lensing* 2017, ISBN 978-1-107-12976-4

8. Feng, J. et. al. *A Global Solution to a Slim Accretion Disk with Radiation-driven Outflows* 2019, ApJ 885, 93

9. GRAVITY Collaboration *Detection of the gravitational redshift in the orbit of the star S2 near the Galactic centre massive black hole* 2018, A&A 615, L15

10. Howil, K. et. al. *Uncovering the Invisible: A Study of Gaia18ajz, a Candidate Black Hole Revealed by Microlensing* 2025, A&A 694, A94

11. ISO-IEC 61966-2-1 *Part 2-1: Colour management — Default RGB colour space - sRGB*

12. Luminet, J.P. *Image of a spherical black hole with thin accretion disk* 1979, A&A 75, 228

13. Marck, J. & Luminet, J.P. *Plongeon dans un trou noir* (fr)

14. Poutanen, J. *Accurate analytic formula for light bending in Schwarzschild metric* 2020, A&A 640, A24

15. Semerak, O. *Approximating Light Rays in the Schwarzschild Field* 2015, ApJ 800, 77

16. The Event Horizon Telescope Collaboration et. al. *First Sagittarius A* Event Horizon Telescope Results. V. Testing Astrophysical Models of the Galactic Center Black Hole* 2022, ApJ 930, L16 https://doi.org/10.3847/2041-8213/ac6672

17. The Event Horizon Telescope Collaboration et. al. *First Sagittarius A* Event Horizon Telescope Results. VIII. Physical Interpretation of the Polarized Ring* 2024, ApJ 964, L26 https://doi.org/10.3847/2041-8213/ad2df1

18. Wardzinski, G. *Radiative processes in accreting black holes* 2002